Pergamon

J Quant. Spectrosc. Radiat. Transfer Vol. 58, No. 4–6. 553–558, 1997

Printed in Great Britain
PII: S0022-4073(97)00061-7 0022-4073/97 $17.00 + 0 00

SIMPLE MULTI-PARTICLE MODEL OF ION DYNAMICAL BROADENING

A. DEREVIANKO† and E. OKS‡§

†Department of Physics, University of Notre Dame, Notre Dame, IN 46556, U.S.A. and
‡Physics Department, 206 Allison Lab., Auburn University, Auburn, AL 36849-5311, U.S.A.

Abstract—The existing analytical models of ion dynamical broadening, while working relatively well at high densities, become progressively more inaccurate at low densities. We have developed a new analytical model that is free from this shortcoming and is also simpler than most of its predecessors. Our model is based on dynamic characteristics of the multi-particle ion microfield introduced by Chandrasekhar and von Neumann. These characteristics are used for separating the entire ensemble of microfields into two parts that act differently on radiating atoms/ions: a dynamic part, that is then treated in the impact approximation, and the remaining part, treated in the quasistatic approximation. It turns out that this model not only is *simpler and faster* than the previous analytical models, but also is practically as *accurate* as simulation models. The comparison with the experiments shows that our model is universal: it yields a good agreement with the experiments over five orders of magnitude density range where the experimental results are available. © 1997 Elsevier Science Ltd. All rights reserved

1. INTRODUCTION

There are two groups of models for the ion dynamical broadening: simulation models (SM) and analytical models (AM) – see, e.g, Ref. 1 and references therein. SM are further subdivided into fully numerical models (where both the plasma and the atomic parts of the problem are treated numerically) and semianalytical models (where only the first part is calculated numerically). SM are slow and expensive. Compared to them, AM, such as the model microfield method (MMM) and the frequency fluctuation model (FFM), are faster and less costly. However, all the models, while working relatively well at high densities, become progressively more inaccurate at low densities. The FFM fails to reproduce the ion impact regime; the MMM reproduces this limit only at densities several orders of magnitude below the correct onset of the ion impact regime.

We have developed a new AM that is free from this shortcoming and is also simpler than most of its predecessors. Our model is based on a more extensive use of stochastic characteristics of the multi-particle ion microfield compared to the MMM. These characteristics are used for separating the entire ensemble of microfields into two parts that act differently on radiating atoms: a dynamic part, that is then treated in the impact approximation, and the remaining part, treated in the quasistatic approximation. It turns out that our model is accurate, being simpler and faster than the MMM. In fact, for high and medium densities our model yields the same results as the SM and the experiments. For lower densities, in distinction to all the previous ion-dynamical models, our model reproduces the ion impact broadening limit [2-4] at the correct onset density and yields results in better agreement with experiments than any of the predecessors.

2. DESCRIPTION OF THE MODEL

The first goal is to divide the ensemble of microfields into the dynamic and quasistatic subensembles and to calculate effective densities N_d and N_q of ions in each subensemble. To achieve this we employ the basic characteristic of the multi-particle ion microfield which is the frequency Ω of the variation of any field component at a fixed value of the field strength:

$$\Omega \equiv [< (\mathrm{d}F_{\parallel}/\mathrm{d}t)^2 >_F + < (\mathrm{d}F_{\perp}/\mathrm{d}t)^2 >_F]^{1/2}/(3^{1/2}F) . \quad (1)$$

§To whom all correspondence should be addressed.

Using the corresponding results by Chandrasekhar and von Neumann [5,6], this frequency can be represented in the form

$$\Omega(\beta) = (15/8)^{1/2}\Omega_0/\beta,\ \beta \le \beta_m,\ \Omega(\beta) = \Omega_0\beta^{1/2},\ \beta \ge \beta_m,$$

$$\Omega_0 = (2.603)^{1/2}N_i^{1/3}(2T_i/M_i)^{1/2},\ \beta_m = (15/8)^{1/3} \approx 1.233\,, \tag{2}$$

where $\beta = F/F_0$ is the reduced field strength, $F_0 \approx 2.603Z_ieN_i^{2/3}$.

The separation procedure combines two well-known criteria: the modulation-type and damping-type methods for determining the boundary between quasistatic and dynamic fields (see, e.g., Ref. 7). In other words, it is based on comparing $\Omega(\beta)$ (Fig. 1, solid line) with both the instantaneous splitting of a hydrogen line $n \to n'$,

$$\omega_\beta \equiv [(n^2 - n'^2)\hbar F_0/m_ee]\beta \tag{3}$$

(Fig. 1, dashed line), and the total damping constant,

$$\gamma = 2(\gamma_i + \gamma_e) \tag{4}$$

(Fig. 1, dotted line), where γ_i and γ_e are the ion and electron impact HWHMs of the line, γ_i being calculated below. Further details on the modulation-type quasistaticity condition are given in Appendix A. After finding the root β' of the equation

$$\Omega(\beta) = \max(\omega_\beta, \gamma)\,, \tag{5}$$

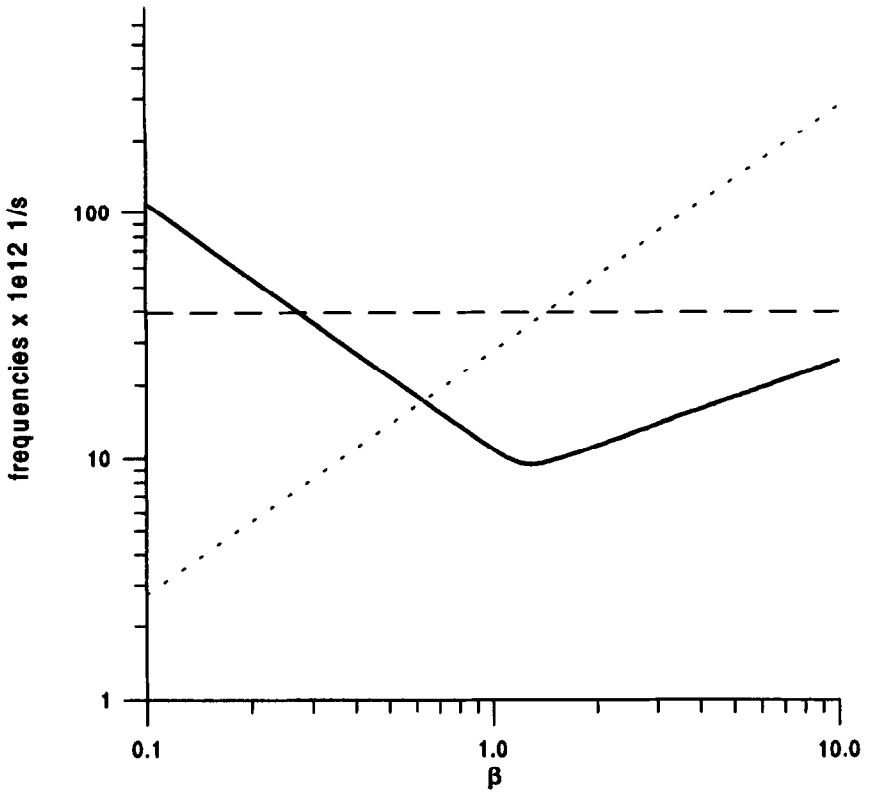

Fig. 1. Comparison of the frequency $\Omega(\beta)$ of the variation of any component of the ion microfield (solid line) with both the instantaneous splitting ω_β of a hydrogen line $n \to n'$ (dashed line) and the summary damping constant $\gamma = 2(\gamma_i + \gamma_e)$ (dotted line). The root of the equation $\Omega(\beta) = \max(\omega_\beta, \gamma)$ separates the dynamic and quasistatic ion subensembles.

we calculate the densities of the dynamic N_d and quasistatic N_q ions as follows:

$$N_d = pN_i,\ N_q = (1-p)N_i,\ p \equiv \int_0^{\beta'} d\beta\ H(\beta)\,, \tag{6}$$

where $H(\beta)$ is the Holtsmark distribution function.

It should be noted that Fig. 1 depicts the situation characteristic of relatively high densities where the $\max(\omega_{\beta'}, \gamma) = \gamma$. This means that the root β' of Eq. (5) is determined by the intersection of the solid curve $\Omega(\beta)$ with the dashed horizontal line γ and that $\beta' \sim 1$ or $\beta' \ll 1$.

For relatively low densities the situation is such that $\max(\omega_{\beta'}, \gamma) = \omega_{\beta'}$. In other words, the root of Eq. (5) in this case is determined by the intersection of the solid curve $\Omega(\beta)$ with the dotted straight line ω_β; the intersection occurs at $\beta' \gg 1$.

At the second stage the goal is to calculate the total damping constant $\gamma = 2(\gamma_i + \gamma_e)$ that includes the ion impact width γ_i due to the dynamic subensemble of the ion density N_d and the electron impact width γ_e. It turns out that for the dynamic ion subensemble the number of ions in the ion Weisskopf sphere is smaller than one not only for the case where the initial density N_i is low but also for high densities N_i. This is due to the fact that in the latter case we have $N_d \ll N_i$. Therefore the ion impact broadening operator Φ_i can be calculated using the standard, binary ion impact theory [2-4] by substituting N_i by N_d.

In order to find the total damping constant for lines with the central (unshifted) Stark component(s), we calculate the following line profile:

$$I_c(\Delta\omega) = (-1/\pi)\mathrm{Re}\sum_{\alpha\alpha'\beta\beta'} d_\alpha^\beta d_{\beta'}^{\alpha'}\{[i\Delta\omega - i\omega_{\alpha\beta}(F_p) + \Phi_i(N_d) + \Phi_e]^{-1}\}_{\alpha'\beta'}^{\alpha\beta}\,, \tag{7}$$

where

$$F_p \approx 1.62F_q \approx 4.21Z_i eN_q^{2/3} \tag{8}$$

is the most probable value of the quasistatic ion field (from the Holtsmark distribution) controlled by the density N_q of the quasistatic ions. As the quasistatic field increases, it provides the transition from the merged to isolated Stark components [7]; in the latter limit the width of the line with the central component(s) is practically determined by the impact width of the central component(s) only.

From the profile given in Eq. (7) we determine the FWHM γ. We note that the obtained total damping constant γ depends on the value of N_d, which in its turn was calculated at the stage 1 using the value of γ. Clearly, this algorithm is an iterative procedure that, fortunately, converges very rapidly.

As for the lines without the central Stark components, we suggest that the total damping constant γ should be determined as the FWHM of the following profile which is due to only homogeneous mechanisms of Stark broadening:

$$I_{un}(\Delta\omega) = (-1/\pi)\mathrm{Re}\sum_{\alpha\alpha'\beta\beta'} d_\alpha^\beta d_{\beta'}^{\alpha'}\{[i\Delta\omega + \Phi_i(N_d) + \Phi_e]^{-1}\}_{\alpha'\beta'}^{\alpha\beta}\,. \tag{9}$$

At the third stage we calculate the final line profile by the formula

$$I(\Delta\omega) = \int_0^\infty d\beta_q\ H(\beta_q)(-1/\pi)\mathrm{Re}\sum_{\alpha\alpha'\beta\beta'} d_\alpha^\beta d_{\beta'}^{\alpha'}\{[i\Delta\omega - i\omega_{\alpha\beta}(\beta_q) + \Phi_i(N_d) + \Phi_e]^{-1}\}_{\alpha'\beta'}^{\alpha\beta}\,, \tag{10}$$

where

$$\beta_q \equiv F/F_q,\quad F_q = 2.603Z_i eN_q^{2/3}\,. \tag{11}$$

The above formalism contains both the ion quasistatic limit at high densities and the ion impact limit at low densities.

Table 1.

N_e	T (K)	MMM [13]	Impact [2-4]	SM [12]	our	Experiment	error (%)
9.27×10^{18}	11600				118	123 [8]	3.7
1.00×10^{17}	10000	4.3		4.6	4.7	4.6 [9-11]	2.0
1.00×10^{16}	10000	1.00		1.15	1.16	1.2 [9-11]	0.9
1.00×10^{15}	10000	0.22		0.28	0.30	0.28 [9-11]	6.5
1.00×10^{14}	10000		0.089	0.051	0.122		
1.35×10^{14}	13500		0.088		0.119	0.14 [14]	15

3. DISCUSSION

Using this model, we calculated Stark profiles of the H_α line and HWHM of these profiles for a broad range of densities from $10^{14}\,cm^{-3}$ to $10^{19}\,cm^{-3}$. The comparison of our results with experimental and previous theoretical results is presented in Table 1, where the last column shows the relative inaccuracy of our results compared to the experiments. The conclusions are the following.

a. Our model is in excellent agreement with experiments [8-11] (1% to 6% accuracy) over the range of densities from $10^{15}\,cm^{-3}$ to $10^{19}\,cm^{-3}$.
b. In this range it yields practically the same accuracy as the SM [12] and a much higher accuracy than the MMM [13], despite being simpler and faster than the MMM.
c. At densities below $10^{15}\,cm^{-3}$, the MMM and even the SM [12] fail to reproduce the ion impact regime [2-4], while this regime is reproduced by our model at these densities.
d. At densities of the order of $10^{14}\,cm^{-3}$, our model is still in good agreement with the experiment [14] (within 15% accuracy), while the SM [12] underestimates the broadening by a factor of 2 or 3. We note that at this density the fine structure contribution of $\approx 15\%$ was subtracted from the experimental HWHM. However, this indicates that one should not expect better than 15% agreement between the calculations based on Coulomb-radiator wave functions and the experimental Stark HWHM. The incorporation of the fine structure into our model will be presented elsewhere.

Thus our analytical model is not only simpler, faster, and much more accurate than the MMM, but is also suitable for a variety of plasmas: it works well over five orders of magnitude density range.

REFERENCES

1. Alexiou, S., *J. Quant. Spectr. Rad. Transfer*, 1995, **54,** 1–26.
2. Stehle, C., Mazure, A., Nollez, G. and Feautrier, N., *Astron. Astrophys.*, 1983, **127,** 263–266.
3. Stehle, C. and Feautrier, N., *J. Phys. B*, 1984, **17,** 1477–1489.
4. Stehle, C. and Feautrier, N., *Ann. Phys. Fr.*, 1984, **9,** 697–704.
5. Chandrasekhar, S. and von Neumann, J., *Astrophys. J.*, 1942, **95,** 489.
6. Chandrasekhar, S. and von Neumann, J., *Astrophys. J.*, 1943, **97,** 1.
7. Lisitsa, V. S., *Sov. Phys. Usp.*, 1977, **20,** 603–630.
8. Böddeker, St., Günter, S., Könies, A., Hitzschke, L. and Kunze, H.-J., *Phys. Rev. E*, 1993, **47,** 2785–2791.
9. Kelleher, D. E., Konjevic, N. and Wiese, W. L., *Phys. Rev. A*, 1979, **20,** 1195.
10. Ehrich, H. and Kelleher, D. E., *Phys. Rev. A*, 1980, **21,** 319.
11. Wiese, W. L., Kelleher, D. E. and Paquette, D. R., *Phys. Rev. A*, 1972, **6,** 1132.
12. Oza, D. H., Greene, R. L. and Kelleher, D. E., *Phys. Rev. A*, 1988, **37,** 531–536.
13. Seidel, J., *Z. Naturforsch.*, 1977, **32, a,** 1207–1214.
14. Weber, E. W., Frankenberger, R. and Schilling, M., *Appl. Phys. B*, 1983, **32,** 63–73.
15. Ispolatov, Ya. and Oks, E., *J. Quant. Spectr. Rad. Transfer*, 1994, **51,** 129–138.

APPENDIX

THE MODULATION-TYPE QUASISTATICITY CONDITION (MQC)

It is well known that any type of MQC is based on the adiabatic approach to the Stark broadening (see, e.g., review[7]). Let us first recall the structure of the adiabatic contribution in the electron broadening and then proceed to the ion broadening.

The old adiabatic theory (presented, e.g., in review [7]) was based on the scalar summation of perturber contributions. An explicit expression for the *vector-summation-based* adiabatic width was given for the first time in a recent paper [15] (where a generalized semiclassical theory of the electron broadening, incorporating both adiabatic and nonadiabatic contributions, was developed). Particularly, in the generalized adiabatic theory presented on p. 135 of Ref. 15, the integration over the impact parameters has the form

$$\int_0^\infty \mathrm{d}\rho\ 2\pi\rho[1-(\rho/\rho_{\mathrm{w},a})\sin(\rho_{\mathrm{w},a}/\rho)]\,, \tag{A1}$$

the adiabatic Weisskopf radius $\rho_{\mathrm{w}\,a}$ being defined by

$$\rho_{\mathrm{w},a}\equiv 2C_{\alpha\beta}/v, \qquad C_{\alpha\beta}\equiv 3X_{\alpha\beta}\hbar/(2m_e), \qquad X_{\alpha\beta}\equiv nq_\alpha - n'q_\beta\,, \tag{A2}$$

where the Stark constant $C_{\alpha\beta}$ of the component $\alpha\leftrightarrow\beta$ is expressed through electric quantum numbers $q_\alpha = n_1 - n_2$ and $q_\beta = n_1' - n_2'$ of the upper and lower Stark sublevels, respectively.

Eq. (A1) shows that the adiabatic Weisskopf radius $\rho_{\mathrm{w},a}$ defined in Eq. (A2) provides a separation between the region of the monotonic behavior of the integrand, i.e., $\rho > \rho_{\mathrm{w},a}$ and the region of the strong oscillations of the integrand, i.e., $\rho < \rho_{\mathrm{w},a}$. Thus the contribution of the former to the adiabatic impact width predominates. The precise definition in Eq. (A2) of the Weisskopf radius following from the generalized theory [15] differs by the factor of 2 from the frequently employed [7] order-of-magnitude definition $\rho_{\mathrm{w},a}^{\mathrm{old}} \sim C_{\alpha\beta}/v$.

Physically the adiabatic Weisskopf radius defined in Eq. (A2) separates the region of the weak modulation of the atomic oscillator from the region of the strong modulation. To obtain the same separation of these two regions in terms of frequencies requires a comparison of two frequencies calculated at the instant of the closest approach of the perturbing electron to the radiator. The first one,

$$\Omega(\rho) = v/\rho\,, \tag{A3}$$

is the frequency of the variation of the electron field. The second frequency is

$$\omega'_\rho = 2C_{\gamma\beta}/\rho^2\,, \tag{A4}$$

the instantaneous splitting of the symmetric pair of lateral Stark components $(n,q)\leftrightarrow(n',q')$ and $(n,-q)\leftrightarrow(n',-q')$. Indeed, the root of the equation $\Omega(\rho)=\omega_\rho$ yields the Weisskopf radius defined in Eq. (A2).

With this as background we derive the MQC for the ion broadening. Let us start from the binary case and then generalize the result for the multi-particle case. For such a generalization to be possible, we change the parametrization of the classical paths of perturbers in the binary case.

In the conventional parametrization used in the impact formalism, a rectilinear path of a perturber $\mathbf{r}(t)=\boldsymbol{\rho}+\mathbf{v}t$ is characterized by the vector of its velocity $\mathbf{v}$ and by the perturber's radius-vector $\boldsymbol{\rho}$ at the instant of the closest approach (so that $\boldsymbol{\rho}\bullet\mathbf{v}=0$). In distinction to this, we characterize a rectilinear path of a perturber $\mathbf{r}(t)=\mathbf{R}+\mathbf{v}t$ by the vector of its velocity $\mathbf{v}$ and by the perturber's radius-vector $\mathbf{R}$ at the instant $t=0$, but *we do not* require $t=0$ to be the instant of the closest approach (so that $\mathbf{R}\bullet\mathbf{v}\neq 0$).

In this parametrization the function describing the phase modulation of the atomic oscillator (see, e.g., Eq. (13) of Ref. 15) can be presented in the form

$$f\equiv\exp\{\mathrm{i}[C_{\alpha\beta}/(Z_i e)]\int_{-\infty}^{+\infty} E_z(t)\,\mathrm{d}t\} = \exp\{[\mathrm{i}\rho_{\mathrm{w},a}/(2R)][2w_z - (\mathbf{w}\bullet\mathbf{u})u_z]/[1-(\mathbf{w}\bullet\mathbf{u})^2]\}\,, \tag{A5}$$

where

$$\mathbf{w}\equiv\mathbf{R}/R, \qquad \mathbf{u}\equiv\mathbf{v}/v\,. \tag{A6}$$

Introducing spherical coordinates θ_R, ϕ_R of the unit vector $\mathbf{w}$ in the reference frame with the polar axis Oz and spherical coordinates θ_v, ϕ_v of the unit vector $\mathbf{u}$ in the reference frame *with the polar axis* $Oz'\|\mathbf{w}$, we obtain

$$f=\exp\{\mathrm{i}D[2\cos\theta_R - \cos\theta_i(\cos\theta_i\cos\theta_R - \sin\theta_i\sin\theta_R\cos\phi)]/(1-\cos^2\theta_i)\}\,, \tag{A7}$$

where

$$D\equiv\rho_{\mathrm{w},a}/(2R), \qquad \phi\equiv\phi_R-\phi_i\,. \tag{A8}$$

The averaging of f over ϕ results in the following:

$$<f>_\phi = J_0[B\sin\theta_R\sin\theta_i\cos\theta_i/(1-\cos^2\theta_i)]\exp[\mathrm{i}D\cos\theta_R(2-\cos^2\theta_i)/(1-\cos^2\theta_i)]\,, \tag{A9}$$

where $J_0(x)$ is the Bessel function. One out of two remaining angular averagings (over $\cos\theta_R$) can also be performed analytically using the standard integral employed in Ref. 15, Eq. (28):

$$\int_0^1 \mathrm{d}t\ (1-t^2)^{-1/2}tJ_0(D_1 t)\cos[D_2(1-t^2)^{1/2}] = G^{-1}\sin G, \qquad G\equiv(D_1^2+D_2^2)^{1/2}\,. \tag{A10}$$

With the help of Eq. (A10), the angular average of f over all three angles reduces to the form

$$<f>_{\mathrm{ang}} = \int_0^1 \mathrm{d}x\ G^{-1}(x)\sin G(x), \qquad G(x)\equiv D(4-3x^2)^{1/2}/(1-x^2)\,. \tag{A11}$$

Eq. (A11) demonstrates that the quantity G (which depends through D on the radiator–perturber distance R) separates the region of the monotonic behavior of the integrand, $G<1$, from the region of the strong oscillations of the integrand, $G>1$. The boundary $G=1$ is equivalent to the following equation:

$$x^4-(2-3D^2)x^2-(4D^2-1)=0\,. \tag{A12}$$

It is easy to see that only at $D < 1/2$ does Eq. (A12) have a real root x_0 falling within the integration limits (from 0 to 1):

$$x_0 = [1 - 3D^2/2 - D(1 + 9D^2/4)^{1/2}]^{1/2} . \tag{A13}$$

At $D > 1/2$, real roots of Eq. (A12) fall beyond the integration limits. This means that at $D > 1/2$ we have function $G(x) > 1$ and, consequently, strong oscillations of the integrand in Eq. (A11) in the entire integration range. In other words, $D = 1/2$ serves as a boundary above which there occurs a significant drop-off of the adiabatic contribution of ions to the broadening. The boundary value $D = 1/2$ corresponds to the radiator–perturber distance

$$R_0 = \rho_{W,a} . \tag{A14}$$

Thus we have found that in the (**R**,**v**)-parametrization of perturber paths, the boundary between the region of the weak modulation of the atomic oscillator and the region of the strong modulation is determined by the adiabatic Weisskopf radius defined in Eq. (A2), the definition containing the factor of 2 compared to the order-of-magnitude estimate [7] $\rho_{W,a}^{old} \sim C_{\alpha\beta}/v$. Therefore, similarly to Eq. (A3) and (A4), the separation of the two regions in terms of frequencies requires a comparison of the frequency of the variation of the ion field,

$$\Omega(\rho) = v/R , \tag{A15}$$

with the instantaneous splitting of the symmetric pair of lateral Stark components,

$$\omega'_R = 2C_{\alpha\beta}/R^2 . \tag{A16}$$

The generalization of the MQC from the binary ion microfield (i.e., caused by the nearest neighbor at a distance R from the radiator) to the multi-particle ion microfield is rather obvious. The frequency of the variation of the multi-particle ion field Ω should be used as in Eq. (1) rather than as in Eq. (A15). For the Holtsmark microfield the explicit expression for $\Omega(\beta)$ is given by Eq. (2), which in the binary limit $\beta > > 1$ reduces to Eq. (A15). The instantaneous splitting of the symmetric pair of lateral Stark components should be employed in the form

$$\omega'_\beta = [3(nq_\alpha - n'q_\beta)\hbar F_0/m_e e]\beta . \tag{A17}$$

The last step is to average the frequency ω'_β over the line space (naturally, it would be required in the binary case as well). This step reduces to averaging the absolute value of the electric quantum number q over all n^2 Stark states of the same principal quantum number:

$$< |q| > = (2/n^2) \sum_{q=1}^{n-1} q(n - q) = (n^2 - 1)/(3n) . \tag{A18}$$

With the help of Eq. (A18), we finally obtain $< \omega'_\beta > \equiv \omega_\beta$ given by Eq. (3).